Geometry-Based Propagation Modeling and Simulation of Vehicle-to-Infrastructure Links

Bengi Aygun*, Mate Boban†, Joao P. Vilela⋆, and Alexander M. Wyglinski*
*Department of Electrical and Computer Engineering, Worcester Polytechnic Institute, Worcester, MA, USA
†Huawei European Research Center, Munich, Germany
⋆CISUC, Department of Informatics Engineering, University of Coimbra, Portugal
Email: {baygun, alexw}@wpi.edu, mate.boban@huawei.com, jpvilela@dei.uc.pt

***Abstract*—Due to the differences in terms of antenna height, scatterer density, and relative speed, V2I links exhibit different propagation characteristics compared to V2V links. We develop a geometry-based path loss and shadow fading model for V2I links. We separately model the following types of V2I links: line-of-sight, non-line-of-sight due to vehicles, non-line-of-sight due to foliage, and non-line-of-sight due to buildings. We validate the proposed model using V2I field measurements. We implement the model in the GEMV^2 simulator, and make the source code publicly available.**

I. Introduction

The National Highway Traffic Safety Administration (NHTSA) announced that connected vehicles will be mandated by 2019, and that these vehicles will support both vehicle-to-vehicle (V2V) and vehicle-to-infrastructure (V2I) communications [1]. Furthermore, Federal Highway Administration (FHWA) released "2015 FHWA Vehicle to Infrastructure Deployment Guidance and Products", a document assisting operators in adapting traffic signals and other roadside devices so they are capable to communicate with the new connected vehicles [2]. V2I communication is envisioned as a key building block for enabling safety and traffic efficiency applications in Europe as well [3], [4].

V2I links differ from V2V links, in terms of antenna height, relative speed, and the scatterer density at the infrastructure end of the link, resulting in significantly different communication performance [5]. The infrastructure component of the link will be located near the roads (*e.g.*, at intersections in cities or on gantries on highways) with antennas configured for Dedicated Short Range Communications (DSRC). These characteristics distinguish V2I communication from refers mobile-to-base station ("cellular") communication, where the base station is located farther away from the road, typically mounted on top of buildings or hills. As such, V2I links do not have the same characteristics as the well studied mobile-to-base station links used in cellular networks, for which models are readily available (*e.g.*, [6]).

Field tests are crucial for the study and evaluation of V2I communications. Gozalvez *et al.* [7] performed comprehensive measurements for different antenna heights, vehicle driving directions, and locations in Bologna, Italy. Measurement results on highways involving an infrastructure near the road such as Roadside Units (RSUs) and an onboard units (OBUs) inside of cars with omni-directional antennas show that environment conditions significantly affect communication performance [8]. Shivaldova [9] *et al.* evaluate the performance of omnidirectional and different types of directional antennas and show that directional antennas possess better performance than omnidirectional antennas if the RSUs with directional antennas are deployed properly so as to not cause interference. The propagation behavior of V2I communications in a highway scenario was measured by Maier *et al.* [10] for multi-antenna systems whereas Shivaldova *et al.* [11] analyzed the performance of single-antenna systems in tunnels.

While field tests provide realistic insights for specific scenarios, simulations are better suited for repeatable, low cost evaluations of protocols and applications for vehicular communications. Current state-of-the-art simulators focus mainly on V2V communications or V2I communications operating in the cellular sense (*e.g.*, LTE communication between mobile terminal and base station). Existing V2I studies either utilize simplified OBU-RSU link behavior (*e.g.*, Paulin *et al.* [12] use NS-3 [13] to regulate the data flow and collection between the OBU and RSUs) or focus on LTE communication (*e.g.*, Altintas *et al.* [14] explored the use of cellular communication to enable "cars as an ICT resource" in the context of future smart cities). Although the literature includes many propagation models and channel simulators for V2V systems [15], [16], there is a noticeable lack of models focused on V2I propagation.

Designing accurate propagation models is critical for realistic evaluation of V2I-enabled applications. Specific considerations for V2I communication include the following:

- V2I systems have unique characteristics in terms of antenna heights, placement of the RSUs, relative speed and locations and statistics of scatterers;
- Various environments (*e.g.*, urban, suburban, highway) causing different attenuation levels at same distances (*i.e.*, affecting path loss and shadowing);
- Specific considerations for small scale fading, due to particular location of antennas on both side of the links.

Following the modeling methodology developed in the GEMV^2 simulator [17], in this paper we characterize the path loss and shadowing for V2I communications and develop model that encompasses different V2I link types; these include

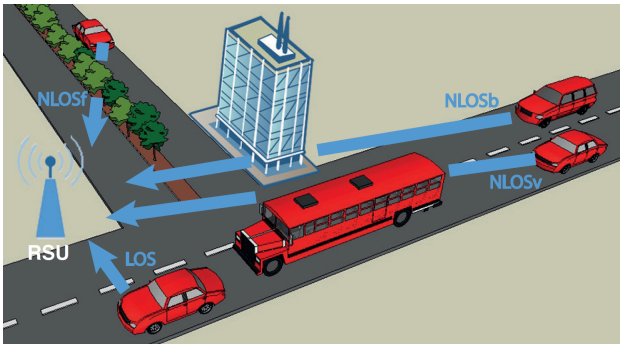

Fig. 1. Vehicle-to-Infrastructure architecture. Link attenuation greatly varies based on the link type: line-of-sight (LOS), non-line-of-sight by vehicles (NLOSv), non-line-of-sight by foliage (NLOSf), non-line-of-sight by buildings (NLOSb).

line-of-sight (LOS) and non-line-of-sight (NLOS) links, with the latter being further classified as NLOS due to obstruction by vehicles (NLOSv), buildings (NLOSb), and foliage (NLOSf), the three main object types affecting propagation in these environments [18]. The link classification is performed by the GEMV^2 simulator: i) using either vehicular mobility data generated by SUMO [19] or real-world traces for vehicle traffic; and ii) outlines of buildings and foliage from Open Street Map [20]. The model is then evaluated against real-world measurements in 5.9 GHz frequency band performed by Gozalvez *et al.* [7].

Compared to the current state-of-the-art, our work contains the following contributions:

- We develop a geometry-based propagation model for each type of V2I link (LOS, NLOSv, NLOSb, and NLOSf);
- We validate the models against independently performed V2I measurements;
- We implement the V2I model in GEMV^2 simulator and make the code freely available.

The rest of the paper is organized as follows: In Section II, we describe the network setup and measurement used for model validation. Section III, details the proposed V2I model and finally, several remarks are provided in Section IV.

II. Network and Measurement Setup

As shown in Fig. 1, LOS of V2I links can be affected by different objects, based on which we classify link types into NLOSv, NLOSf, and NLOSb. We employ real world measurements to : i) extract the large and small scale received power variation parameters; and ii) validate the accuracy of proposed model. We use freely available data from a V2I measurement campaign in 5.9 GHz frequency band performed in the city center of Bologna, Italy [7]. For these measurements, 10 RSUs are deployed throughout the city so as to encompass different conditions in an urban environment. In Fig. 2, the RSUs that are used in this paper and corresponding propagation power levels are depicted. In Fig. 2(a), the OBU approaches the RSU in a straight street which is 500 m long. At each time step the received power is recorded. The levels of received power are shown with colors varying from red to blue, respectively

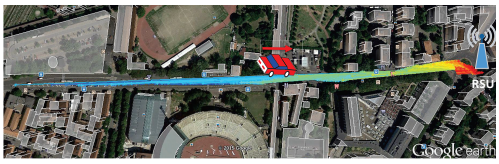

(a) LOS and NLOSv experiment region

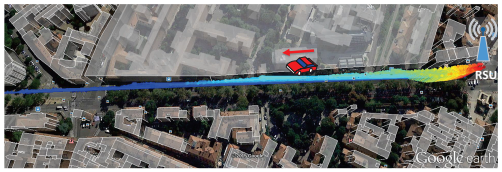

(b) NLOSf experiment region

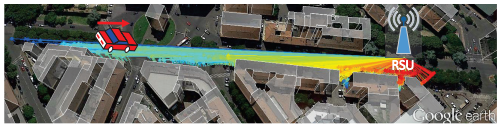

(c) NLOSb experiment region

Fig. 2. Locations of RSUs for selected scenarios representing different link types in the measurement campaign by Gozalvez et al [7].

corresponding to high and low received power. The same setup is also used for NLOS due to heavy vehicle obstacles. In this experiment, the vehicle with OBU approaches the RSU while a heavy vehicle drives right in front of the OBU, thus breaking the direct LOS link. In Fig. 2(b), the RSU is located in a region surrounded by foliage. The street is curve-shaped right in front of the RSU, which is itself surrounded by trees. Hence, the vegetation limits the reception of signals from the RSU, causing extra attenuation. In Fig. 2(c), the RSU is located near a building and the OBU approaches the RSU on the road in front of the building, so that the building breaks the direct link. We propose a model that separately models all these link types and evaluate it against real-world measurements depicted in Fig. 2.

III. Description of V2I Channel Model and Its Validation

In this section, we describe the models for different types of V2I links. For each link type, we define large-scale attenuation effects through a characterization of its unique link properties. The difference to V2V links is also pointed out, and the results are compared against the real world measurements in Bologna [7]. In addition to comparing the proposed model against measurements, we also depict free space path loss as a reference point for the reader (*i.e.,* not as a representative model for all of the link types)..

A. Line-of-Sight V2I links (LOS)

To characterize LOS links, we resort to a two-ray ground reflection model described as follows [21]:

$$|E_{\mathrm{TOT}}| = \frac{E_0 d_0}{d_{\mathrm{LOS}}} cos\left(w_c\left(t - \frac{d_{\mathrm{LOS}}}{c}\right)\right) \\ R_{\mathrm{ground}} \frac{E_0 d_0}{d_{\mathrm{ground}}} cos\left(w_c\left(t - \frac{d_{\mathrm{ground}}}{c}\right)\right) \quad (1)$$

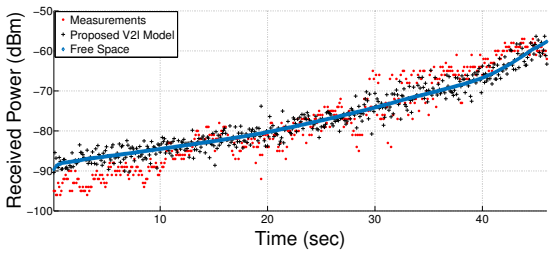

(a) LOS V2I Links: Measurement 1

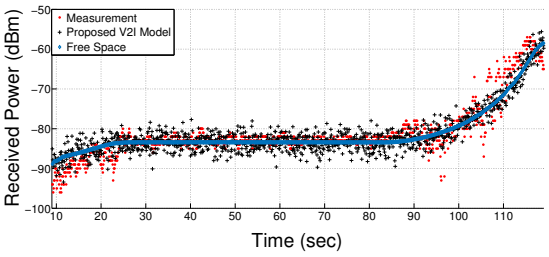

(b) LOS V2I Links: Measurement 2

Fig. 3. LOS V2I Links: OBU monotonically approaches the RSU at each time step for both measurements. Both results generated by the model and measured data have a pattern similar to free space path loss since the link type is LOS. Model vs Measurements: mean absolute error: 3.16 mean; standard deviation: 2.84.

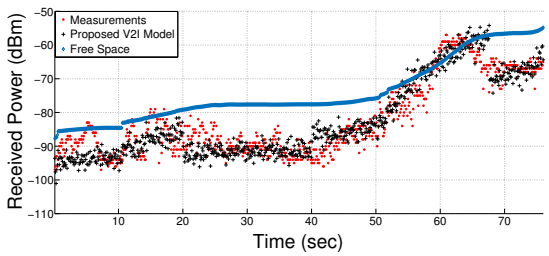

(a) NLOSv V2I: Measurement 1

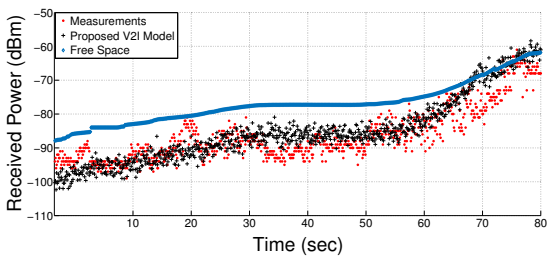

(b) NLOSv V2I: Measurement 2

Fig. 4. NLOSv V2I links: comparison of field measurements and simulated results. OBU approaches to RSU at each time step while the heavy vehicle is driving right front of the OBU. Model vs Measurements: mean absolute error: 3.98 mean; standard deviation: 3.47.

where the reflection coefficient R_{ground} and distance d_{ground} for the ground-reflected ray are calculated according to the exact antenna heights, w_c is the carrier frequency in radian. Since the antenna height of the RSU is higher than the OBU, there are fewer scatterers that are also distributed more isotropically than in case of V2V, thus resulting in less variation due to multipath. In Fig. 3, the OBU approaches the RSU. The same experiment is performed two times. In the first measurement, the OBU approaches the RSU during 450 time steps, so that received power monotonically increases (Fig. 3(a)). In the second measurement, the OBU moves around the RSU by keeping a steady distance throughout 500 time steps and then approaching the RSU, thus leading to increased received power (Fig. 3(b)). As expected, both model and measured data follow a pattern similar to the free space path loss model.

B. Non-Line-of-Sight V2I Links due to Vehicles (NLOSv)

Due to higher antenna heights of RSUs, the impact of vehicles as obstacles in V2I is not as pronounced as in V2V communication [18]. However, vehicles – particularly large ones like buses and trucks – still have a strong impact on V2I communication. When a link between RSU and OBU is blocked by one or more vehicles, additional attenuation can be modeled as (multiple) knife-edge diffraction [18]. According to the knife-edge model, the additional attenuation A can be computed as follows:

$$A=\begin{cases}6.9+20log_{10}\left[\sqrt{(v-0.1)^2+1}+v-0.1\right] & v>0.7\\ 0 & \text{otherwise}\end{cases} \quad (2)$$

where $v=\sqrt{2}H/r_f$, H is the height difference between obstacle and OBU antenna, r_f is the Fresnel ellipsoid radius. In Fig. 4, field measurements for the RSU deployed in Bologna are compared with the considered NLOSv model. During the measurement, there is a heavy vehicle in front of the OBU as it approaches the RSU. The same experiment is performed twice, with the first lasting 700 (Fig. 4(a)) and the other one 800 time steps (Fig. 4(b)). The distance between the heavy vehicle and the OBU varies between 5 and 25 m during the measurements. We can observe that the proposed model matches measured data well, with mean absolute error of 3.98 and standard deviation of 3.47 over the two experiments. The good match shows the flexibility of the knife-edge model, which, unlike stochastic models, takes into account the heights of antennas and obstructing objects to calculate the link attenuation.

C. Non-Line-of-Sight V2I links due to Foliage (NLOSf)

NLOSf links are modeled by using the empirical derivation given by Goldhirsh *et al.* [22], where the attenuation caused by foliage is defined as mean excess loss (MEL) per meter as follows:

$$\text{MEL}=0.79f^{0.61} \quad (3)$$

where f is the carrier frequency, *i.e.* 5.9 GHz for 802.11p-based communication. MEL is multiplied with the length of propagation through foliage. Note that the vegetation significantly affects received power of V2I links only if it is high relative to the OBU-RSU link (otherwise, there is only the effect of scattering off foliage). In Fig. 5, field measurements for the RSU deployed in Bologna are compared with the

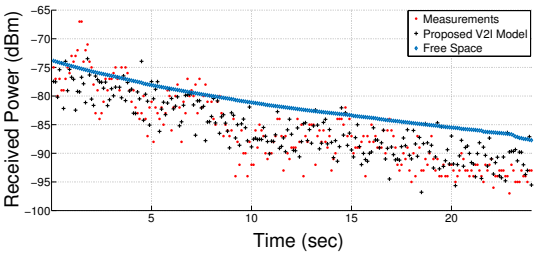

(a) NLOSf V2I links: Measurement 1

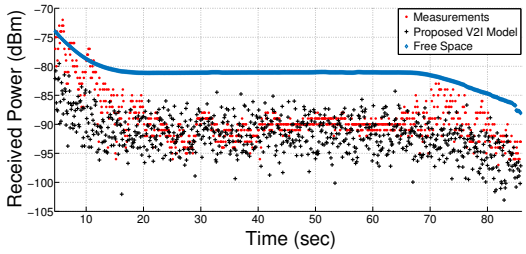

(b) NLOSf V2I links: Measurement 2

Fig. 5. NLOSf V2I links: comparison of field measurements and simulated results. Model vs Measurements: mean absolute error: 4.14 mean; standard deviation: 3.64.

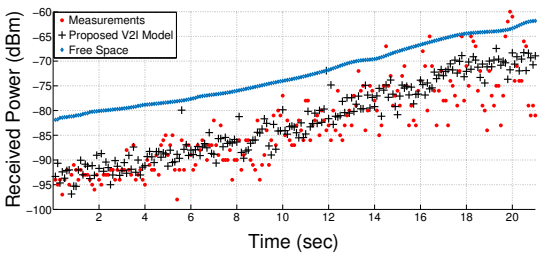

(a) NLOSb V2I: Measurement 1

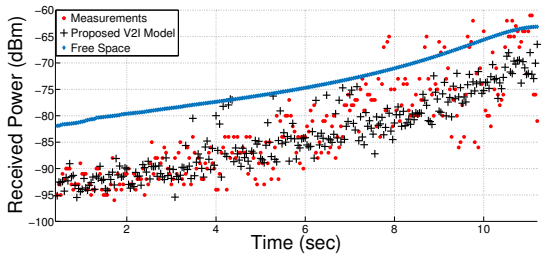

(b) NLOSb V2I: Measurement 2

Fig. 6. NLOSb V2I links: comparison of field measurements and simulated results. Model vs Measurements: mean absolute error: 5.03 mean; standard deviation: 5.79.

proposed model. In this experiment, the RSU is located on a road that has a curve surrounded by trees; once the OBU moves behind the curve, the direct link becomes obstructed by trees. The measurement in the location shown in Fig. 2(b) is performed two times. In the first measurement, the OBU drives away from the RSU during 350 time steps, so that the received power decreases largely monotonically (Fig. 5(a)). In the second measurement (Fig. 5(b)), the OBU moves away from RSU; between time step 200 and 700, the speed is very low (under 1 km/h), which is reflected in almost stable received power. The transmission distance through foliage (and thus the attenuation) gradually increases in the first measurement, while it remains stable in the second measurement, as evidenced relative to the free space path loss. Fig. 5 shows that the proposed model can model the foliage-obstructed V2I links well.

D. Non-Line-of-Sight V2I links due to Buildings Obstacles (NLOSb)

Since the large scale effect of buildings is similar for V2V and V2I links, for the attenuation on V2I NLOSb link, we used the model for V2V NLOSb from GEMV^2 simulator [16], with modified small scale signal variation parameters, which were extracted from V2I measurements [7]. In the model, the attenuation due to buildings is estimated as the maximum received power between: i) the joint effect of single-interaction diffractions and reflections; and ii) the log distance path loss model with a comparatively high path loss exponent (for details, see [16]). In Fig. 6, the field measurements for the RSU deployed in Bologna (shown in Fig. 2(c)) are compared with the proposed model. In this measurement, the RSU is located near a building and the OBU approaches it through the street in front of the building. Therefore, the nearby building slightly breaks the direct link between OBU and RSU, resulting in a moderate attenuation due to the building. The same experiment is performed two times. We can observe that the proposed model result matches measured data with mean absolute error of 5.03 and standard deviation of error of 5.79.

E. Small-scale Variation of Received Power

For each V2I link type, Table I shows the minimum and maximum small scale received power variation value extracted from the measurements as follows: for each 5-meter distance bin with at least 20 data points, we obtain the standard deviation of the received power for all data points. As described in [16], these limits are then used to interpolate the specific value of small scale variation of received power based on the stochastic model taking into account the number and area of objects around RSU and OBU. While the values in Table I are specific for the environment where the measurements were collected and should be used with caution in other environments, the relationship between the values gives an insight into the difference that small scale power variation experiences for different link types. As expected, LOS V2I links have the least variation, since the dominant LOS ray contributes the most power at the receiver. NLOSb links, on the other hand, have the largest variation due to the strong variation of the level of LOS obstruction by buildings. Also, note that more severe NLOSb scenarios than those in the analyzed measurements are easily conceivable; *e.g.*, RSU and OBU located on parallel streets obstructed by rows of buildings. For such cases, the

TABLE I
PARAMETER SETTINGS FOR V2I MODEL

Standard Deviation of Received Power per Bin	LOS	NLOSv	NLOSf	NLOSb
Mean (dBm)	2.1793	2.6080	2.4004	3.3017
Min (dBm)	0.7648	0.9621	1.5158	1.8694
Max (dBm)	6.9032	5.9743	5.2553	7.3640
Path Loss Exponent	2	2 plus knife-edge	2 plus MEL	2.5 (slight NLOSb) 3 (strong NLOSb)

small scale signal variation statistics need to be measured and included in simulations.

The mean and standard deviation of error in Figs. 3-6 show that the model agrees well with the measurements. We note that the mean error is lower-bounded by the mean standard deviation of received power per bin (see Table I) used to generate small scale variations for each link type [23], [24]. Furthermore, the mean and standard deviation of the error is observed on LOS, NLOSv, NLOSf, NLOSb from the lowest to the highest respectively. This result is expected, since the complexity of scatterer characterization involved in subsequent links is increasing [25]. Furthermore, the results show that the scatterers have less of an impact on the received power, with all link types showing significantly lower standard deviation of received power per bin than the same V2V link types due to the height and position of RSUs [16], [26].

IV. CONCLUSION

We developed, validated, and implemented a V2I propagation model that be used in system level vehicular communication simulators. We separately modeled each of the following V2I link types: line-of-sight, non-line-of-sight due to vehicle obstacles, foliage obstacles, and building obstacles (LOS, NLOSv, NLOSf, and NLOSb, respectively). The proposed models, while adapted from existing work on V2V communication, have characteristics that are specific for V2I communication, such as lower values of small scale received power variation and reduced, but not negligible, impact of vehicular obstructions. To be useful for system level simulations, the four V2I link types were first identified by a simulator such that they can be modeled appropriately. For this purpose, we implemented the V2I models in the GEMV^2 simulator [16], using SUMO for vehicular mobility, and building and foliage data from OpenStreetMap to distinguish different link types. We compared the model with a set of V2I measurements collected in Bologna [7] in terms of received power and showed that the proposed model can properly represent each of the four V2I link types. The source code of the V2I model is freely available as part of the GEMV^2 simulator package [17].

REFERENCES

[1] Planning Future Transportation: Connected Vehicles and ITS. [Online]. Available: http://www.its.dot.gov/factsheets/pdf/PlanningFutureTransportation_FactSheet.pdf

[2] 2015 FHWA Vehicle to Infrastructure Deployment Guidance and Products. [Online]. Available: http://www.its.dot.gov/meetings/pdf/V2I_DeploymentGuidanceDraftv9.pdf

[3] ETSI TC ITS, "Intelligent Transport Systems (ITS); Vehicular Communications; Basic Set of Applications; Part 1: Functional Requirements," Tech. Rep. ETSI TR 102 637-1 V1.1.1, Sep. 2010.

[4] Cooperative ITS Corridor Joint Deployment. [Online]. Available: https://www.bmvi.de/SharedDocs/EN/Anlagen/VerkehrUndMobilitaet/Strasse/cooperative-its-corridor.pdf?__blob=publicationFile

[5] M. Boban and P. d'Orey, "Measurement-based Evaluation of Cooperative awareness for V2V and V2I Communication," in *2014 IEEE Vehicular Networking Conference (VNC)*, Dec 2014, pp. 1–8.

[6] Information Society Technologies, " Final Report on Link Level and System Level Channel Models," Tech. Rep. IST-2003-507581 WINNER I, D5.4,, 2005.

[7] J. Gozalvez, M. Sepulcre, and R. Bauza, "IEEE 802.11p Vehicle to Infrastructure Communications in Urban Environments," *IEEE Communications Magazine*, vol. 50, no. 5, pp. 176–183, May 2012.

[8] V. Shivaldova, A. Winkelbauer, and C. Mecklenbrauker, "Vehicular Link Performance: From Real-World Experiments to Reliability Models and Performance Analysis," *Proceedings of IEEE Vehicular Technology Magazine*, vol. 8, no. 4, pp. 35–44, Dec 2013.

[9] V. Shivaldova, A. Paier, D. Smely, and C. Mecklenbrauker, "On Roadside Unit Antenna Measurements for Vehicle-to-Infrastructure Communications," in *Proceedings of IEEE International Symposium on Personal, Indoor and Mobile Communications (PIMRC)*, Sydney, Australia, September 2012, pp. 1–5.

[10] G. Maier, A. Paier, and C. Mecklenbrauker, "Performance Evaluation of IEEE 802.11p Infrastructure-to-Vehicle Real-World Measurements with Receive Diversity," in *Proceedings of the 8th International Wireless Communications and Mobile Computing Conference (IWCMC)*, Limassol, Cyprus, August 2012.

[11] V. Shivaldova, G. Maier, D. Smely, N. Czink, A. Alonso, A. Winkelbauer, A. Paier, and C. Mecklenbrauker, "Performance Evaluation of IEEE 802.11p Infrastructure-to-Vehicle Tunnel Measurements," in *Proceedings of International Wireless Communications and Mobile Computing Conference (IWCMC)*, Istanbul, Turkey, July 2011, pp. 1–5.

[12] T. Paulin and S. Bessler, "Controlled Probing - A System for Targeted Floating Car Data Collection," in *IEEE Intelligent Transportation Systems (ITSC)*, Oct 2013, pp. 1095–1100.

[13] NS-3. [Online]. Available: http://www.nsnam.org/

[14] O. Altintas, F. Dressler, F. Hagenauer, M. Matsumoto, M. Sepulcre, and C. Sommer, "Making Cars a Main ICT Resource in Smart Cities," in *Proceedings of First International Workshop on Smart Cities and Urban Informatics*, Hong Kong, China, April 2015.

[15] B. Aygun and A. Wyglinski, "Channel Modeling of Decode-and-Forward Relaying VANETs," in *IEEE 80th Vehicular Technology Conference*, Sept 2014, pp. 1–5.

[16] M. Boban, J. Barros, and O. Tonguz, "Geometry-Based Vehicle-to-Vehicle Channel Modeling for Large-Scale Simulation," *IEEE Transactions on Vehicular Technology*, vol. 63, no. 9, pp. 4146–4164, Nov 2014.

[17] GEMV2I. [Online]. Available: http://vehicle2x.net/

[18] M. Boban, T. Vinhoza, M. Ferreira, J. Barros, and O. Tonguz, "Impact of Vehicles as Obstacles in Vehicular Ad Hoc Networks," *IEEE Journal on Selected Areas in Communications*, vol. 29, no. 1, pp. 15–28, January 2011.

[19] Simulation of Urban MObility (SUMO). [Online]. Available: http://sumo.dlr.de/wiki/Main_Page

[20] Open Street Map. [Online]. Available: http://www.openstreetmap.org

[21] T. S. Rappaport, *Wireless Communications: Principles and Practice*. Prentice Hall, 1996.

[22] J. Goldhirsh and W. J. Vogel, "Handbook of Propagation Effects for Vehicular and Personal Mobile Satellite Systems – Overview of Experimental and Modeling Results," The Johns Hopkins University, Tech. Rep. A2A-98-U-0-021 (APL), EERL-98-12A (EERL), December 1998.

[23] J. Karedal, F. Tufvesson, T. Abbas, O. Klemp, A. Paier, L. Bernado, and A. Molisch, "Radio Channel Measurements at Street Intersections for Vehicle-to-Vehicle Safety Applications," in *IEEE 71st Vehicular Technology Conference*, May 2010, pp. 1–5.

[24] J. K. Taimoor Abbas, Katrin Sjoberg and F. Tufvesson, "A Measurement Based Shadow Fading Model for Vehicle-to-Vehicle Network Simulations," *International Journal of Antennas and Propagation*, 2015.

[25] W. Viriyasitavat, M. Boban, H.-M. Tsai, and A. Vasilakos, "Vehicular Communications: Survey and Challenges of Channel and Propagation Models," *IEEE Vehicular Technology Magazine*, vol. 10, no. 2, pp. 55–66, June 2015.

[26] L. Cheng, B. Henty, D. Stancil, F. Bai, and P. Mudalige, "Mobile Vehicle-to-Vehicle Narrow-Band Channel Measurement and Characterization of the 5.9 GHz Dedicated Short Range Communication (DSRC) Frequency Band," *IEEE Journal on Selected Areas in Communications*, vol. 25, no. 8, pp. 1501–1516, Oct 2007.